The International Journal of Advanced Manufacturing Technology (2018) 99:1673–1686
https://doi.org/10.1007/s00170-018-2580-y

ORIGINAL ARTICLE

Analysis of *Q*-factor's identification ability for thin-walled part flank and mirror milling chatter

Haibo Liu[1] · Qile Bo[1,2] · Hao Zhang[1] · Yongqing Wang[1]

Received: 29 March 2018 / Accepted: 14 August 2018 / Published online: 25 August 2018

Abstract
Due to its relatively high gravity material removal, the thin-walled part machining would go through a complex process, from stable to unstable and/or reverse repeatedly. As a result, the monitored signals generally exhibit full-oscillatory behaviors, which require that the chatter indicators should meet the dynamic conditions. However, the conventional indicators, including time domain indicators and time-frequency domain indicators, could only capture the state mutation point in the continuous process. In this paper, a novel chatter indicator, *Q*-factors, is proposed for chatter detection. The relationship between *Q*-factor and signal oscillatory behavior is illustrated from the perspective of signal's frequency characteristics and tool-workpiece system's response. Chatter indicator's identification ability for thin-walled part flank and mirror milling is analyzed, i.e., its ability to express characteristics of machining state, sensibility to change machining state, and its chatter-related information inclusion. It can be indicated that as a multi-dimensional indicator, *Q*-factor can be used to identify chatter-related signal component and quantify the level of chatter simultaneously. The value of *Q*-factor exhibits obvious difference between stable state and chatter state. The obvious mutation at the place where the machining state changes will supply more useful and effective information for the following chatter prediction and suppression before the chatter is completely developed.

Keywords Identification ability · *Q*-factor · Thin-walled parts · Chatter · Flank milling · Mirror milling

1 Introduction

For thin-walled part machining, chatter is always a thorny and complex problem which would do great harm to surface quality, escalate tool wear, and limit productivity [1]. Online monitoring based on process variables, including cutting force, acceleration, vibration, sound, torque, and so on, has been an effective way for chatter detection and machining state diagnosis [2]. Whatever kind of process variable signal can apply, the dimensional or non-dimensional chatter indicator varying with machining state will be the key to the identification of the machining chatter of thin-walled parts.

✉ Qile Bo
baoqile1988@mail.dlut.edu.cn

[1] Key Laboratory for Precision and Non-traditional Machining Technology of Ministry of Education, Dalian University of Technology, Dalian 116024, China

[2] School of Mechanical Engineering, Dalian University of Technology, Linggong Road No. 2, Ganjingzi District, Dalian City, Liaoning Province, China

Generally, for the common tool-workpiece system with high rigidity, the corresponding chatter frequency is generally fixed around a series of constant frequencies (commonly the natural frequencies) [3]. But for the thin-walled part machining, some factors, such as material removal [4–6] and cutting tool position along toolpath [7–11], should be considered as well. These factors indicate participation of time-varying workpiece modes at different positions and variation process of machining. These time-varying modal parameters, coupled with the cutting movement of the cutter, make the measured vibration signal more aperiodic and complex. Therefore, in order to detect or identify chatter effectively and timely, the chatter indicator should possess the following characteristics:

- The indicator should contain the chatter-related signal information, i.e., the time-varying modal parameters and the chatter level. In other words, it can not only reflect the change of modal parameters and locate the chatter-related signal component but also quantify the level of chatter.
- The indicator should be sensitive to the exchange of the machining state, and its value or variation should show great correlation with the machining state.

- The indicator can be used for different machining processes without the time-consuming recalibration process. Therefore, its value should be much less susceptible to cutting condition changes, i.e., its variation range is independent of process parameters [12].

Until now, numerous indicators have been proposed to identify machining chatter or evaluate the chatter level. Generally, they can be divided into time domain indicators and time-frequency domain indicators according to the time-frequency characteristics of adopted signals. The time domain indicators mainly include standard deviation [13–17], root mean square error [13, 15, 18], peak value [13–15, 18], crest factor [13, 14, 19], coefficient of variation [20, 21], kurtosis [19, 22, 23], energy of signal [23–25], impulse factor [26, 27], skewness [14, 15, 17, 23], clearance factor [27], shape factor [27], permutation entropy [28, 29], and so on. By contrast, the time-frequency domain indicators try to reveal the characteristics in time-frequency domain. Besides the common indicators including amplitude, energy of dominant spectral spectrum [13, 18, 30–32], standard deviation, root mean square, skewness, and kurtosis of the power spectrum distribution [18], some complex indicators like complexity [33], spectral kurtosis [34, 35], and power spectral entropy [36] are more and more widely used in chatter diagnosis and detection. Meanwhile, with the development of advanced signal processing methods including wavelet transform (WT) [24], Hilbert-Huang transform (HHT) [37, 38], independent component analysis (ICA) [39], singular spectrum analysis (SSA) [40], blind source separation (BSS) [41, 42], and so on, many quantities have derived from these methods and been applied to characterize chatter behaviors in different perspectives.

But not all the aforementioned indicators can meet the characteristics mentioned above and work effectively for thin-walled part machining. For the time domain indicators, they can reveal the signal characteristics in time domain but do not contain the information in frequency domain. Therefore, they can only be used to quantify the level of chatter in time domain, but cannot reveal the time-varying process of modal parameters and locate the chatter-related signal component. For time-frequency domain, some indicators corresponding to multiple frequency bands have a great enlargement within the machining process. It is inaccurate and curt to identify the signal component with obvious enhancement of aforementioned indicators as the chatter-related one. Besides, for some indicators, the exchange within the machining process is smooth-going and not dramatic. There is no remarkable mutation and the threshold of chatter identification is ambiguous, which makes the machining state diagnosis difficult. Moreover, few researches could detect the chatter-related signal component in thin-walled machining process when the frequencies and vibration modes vary with time, which is especially important for the regeneration chatter state where the chatter frequency and tool passing frequency are close.

Therefore, a physical meaningful indicator including the information about the time-varying modal parameters and vibration characteristics will be proper for chatter identification of thin-walled parts. As a quantification of the oscillatory nature of a single transient, Q-factor affects the oscillatory behavior of the wavelet basis function and has been used for tunable Q-factor wavelet transform (TQWT) [43, 44]. By adjusting the Q-factor, the oscillatory behavior of the wavelet basis can be chosen to match the oscillatory behavior of the signal of interest. The relationship between signal's oscillatory behavior and Q-factor has been illustrated in [41, 43–46]. For the vibration signal in machining process, the signal in stable state exhibits periodic and high oscillatory behavior with a high value of Q-factor. But the signal in unstable state shows transient and low oscillatory behavior with a low value of Q-factor. Besides, Q-factor estimates the state transmission from the local waveform point of view, containing information about both of center frequency and bandwidth. The center frequency can be used for characterizing the time-varying modal parameters, and the value of Q-factor can be used for the quantification of the vibration level, which makes the Q-factor suitable for chatter-related signal component identification for thin-walled part machining.

In this paper, Q-factor is selected for chatter identification and its identification ability for thin-walled part machining will be analyzed. In order to illustrate the physical meaning of Q-factor in thin-walled part machining process, the relationship between Q-factor and the signal oscillatory behavior is proposed in Section 2. Then, the calculation procedure of Q-factor based on linear predictive analysis is discussed. Finally, the identification ability in terms of the ability to express characteristics of machining state, the sensibility to the change of machining state, and chatter-related information inclusion between the common indicators and Q-factors are analyzed with two different thin-walled part machining methods.

2 Relationship between Q-factor and the signal oscillatory behavior

Q-factor is denoted by the ratio of the center frequency to the bandwidth of an oscillatory pulse signal,

$$Q = \frac{f_0}{Bw} \tag{1}$$

where f_0 represents the center frequency and Bw represents the bandwidth of one impulse signal.

The value of Q-factor reflects the oscillatory properties of the signal. The relationship between Q-factor and signal oscillatory behavior is shown in Fig. 1. For the periodic harmonic signal shown in Fig. 1a, b, the frequency band is narrow and

the Q-factor is higher based on the definition. In this case, the energy of the signal dissipates at a low rate and the signal exhibits better frequency aggregation. Comparatively, for the transient pulse signal shown in Fig. 1c, d, the frequency bandwidth is wide and the Q-factor is lower. It means that the energy of the signal dissipates at a high rate and the signal exhibits worse frequency aggregation. In a sense, the Q-factor counts the number of oscillation in temporal response [44].

The relationship between Q-factor and machining signal oscillatory behavior can also be expressed with the machining dynamics. The dynamic motion equation of three DOF systems can be described as

$$M\begin{bmatrix}\ddot{x}(t)\\ \ddot{y}(t)\\ \ddot{z}(t)\end{bmatrix}+C\begin{bmatrix}\dot{x}(t)\\ \dot{y}(t)\\ \dot{z}(t)\end{bmatrix}+K\begin{bmatrix}x(t)\\ y(t)\\ z(t)\end{bmatrix}=\begin{bmatrix}F_x\\ F_y\\ F_z\end{bmatrix} \tag{2}$$

where $M=\begin{bmatrix}M_{xx} & M_{xy} & M_{xz}\\ M_{yx} & M_{yy} & M_{yz}\\ M_{zx} & M_{zy} & M_{zz}\end{bmatrix}$, $C=\begin{bmatrix}C_{xx} & C_{xy} & C_{xz}\\ C_{yx} & C_{yy} & C_{yz}\\ C_{zx} & C_{zy} & C_{zz}\end{bmatrix}$, $K=\begin{bmatrix}K_{xx} & K_{xy} & K_{xz}\\ K_{yx} & K_{yy} & K_{yz}\\ K_{zx} & K_{zy} & K_{zz}\end{bmatrix}$ are the mass coefficients, damping coefficients, and stiffness coefficient of the cutting system respectively. $M_{xx}=m_x, M_{yy}=m_y, M_{zz}=m_z, C_{xx}=2m_x\zeta_x\omega_x, C_{yy}=2m_y\zeta_y\omega_y, C_{zz}=2m_z\zeta_z\omega_z, K_{xx}=m_x\omega_x^2, K_{yy}=m_y\omega_y^2$, and $K_{zz}=m_z\omega_z^2$ are the corresponding mode coefficients in X, Y, and Z directions. m_x, m_y, and m_z; ζ_x, ζ_y, and ζ_z; ω_x, ω_y, and ω_z are the modal mass, relative damping, and angular natural frequency. The coupling structural mode coefficients of $M_{xy}, M_{xz}, M_{yx}, M_{yz}, M_{zx}, M_{zy}, C_{xy}, C_{xz}, C_{yx}, C_{yz}, C_{zx}, C_{zy}, K_{xy}, K_{xz}, K_{yx}, K_{yz}, K_{zx}$, and K_{zy} can be set as zero as structural mode coupling effect is neglected. $[F_x\ F_y\ F_z]^T$ are the corresponding cutting forces in X, Y, and Z directions, where,

$$\begin{bmatrix}F_x\\ F_y\\ F_z\end{bmatrix}=\begin{bmatrix}-a_ph_{xx}(t) & -a_ph_{xy}(t) & -a_ph_{xz}(t)\\ -a_ph_{yx}(t) & -a_ph_{yy}(t) & -a_ph_{yz}(t)\\ -a_ph_{zx}(t) & -a_ph_{zy}(t) & -a_ph_{zz}(t)\end{bmatrix}\begin{bmatrix}x(t)\\ y(t)\\ z(t)\end{bmatrix}+\begin{bmatrix}a_ph_{xx}(t) & a_ph_{xy}(t) & a_ph_{xz}(t)\\ a_ph_{yx}(t) & a_ph_{yy}(t) & a_ph_{yz}(t)\\ a_ph_{zx}(t) & a_ph_{zy}(t) & a_ph_{zz}(t)\end{bmatrix}\begin{bmatrix}x(t-T)\\ y(t-T)\\ z(t-T)\end{bmatrix}$$

a_p is the axial cutting depth. $[x(t)\ y(t)\ z(t)]^T$, $[\dot{x}(t)\ \dot{y}(t)\ \dot{z}(t)]^T$, and $[\ddot{x}(t)\ \ddot{y}(t)\ \ddot{z}(t)]^T$ are the vibration displacement, vibration speed, and vibration acceleration in X, Y, and Z directions considering the regenerative effect. T is the tool passing period. $h_{xx}(t)$, $h_{xy}(t)$, $h_{xz}(t)$, $h_{yx}(t)$, $h_{yy}(t)$, $h_{yz}(t)$, $h_{zx}(t)$, $h_{zy}(t)$, and $h_{zz}(t)$ are the cutting force coefficients. Applying the Laplace transform to Eq. (2) gives

$$\left(Ms^2+Cs+K\right)\begin{bmatrix}x(s)\\ y(s)\\ z(s)\end{bmatrix}=\begin{bmatrix}F_x(s)\\ F_y(s)\\ F_z(s)\end{bmatrix} \tag{3}$$

According to the definition of the system transfer function and applying $s=i\omega$, the transfer functions in X, Y, and Z directions can be obtained,

$$\begin{cases}G_{xx}(i\omega)=\dfrac{1}{k_x}\dfrac{1}{-\left(\frac{\omega}{\omega_x}\right)^2+2i\xi_x\left(\frac{\omega}{\omega_x}\right)+1}\\ G_{yy}(i\omega)=\dfrac{1}{k_y}\dfrac{1}{-\left(\frac{\omega}{\omega_y}\right)^2+2i\xi_y\left(\frac{\omega}{\omega_y}\right)+1}\\ G_{zz}(i\omega)=\dfrac{1}{k_z}\dfrac{1}{-\left(\frac{\omega}{\omega_z}\right)^2+2i\xi_z\left(\frac{\omega}{\omega_z}\right)+1}\end{cases} \tag{4}$$

According to the dynamic equation for the thin-walled part machining process, the regenerative displacement can be expressed as [47]

$$\begin{cases}\Delta x(i\omega t)=x(i\omega t)-x_0(i\omega t)=\left(1-e^{-i\omega t}\right)\cdot G_{xx}(i\omega)\cdot|F_x(t)|\cdot e^{i\omega}\\ \Delta y(i\omega t)=y(i\omega t)-y_0(i\omega t)=\left(1-e^{-i\omega t}\right)\cdot G_{yy}(i\omega)\cdot|F_y(t)|\cdot e^{i\omega}\\ \Delta z(i\omega t)=z(i\omega t)-z_0(i\omega t)=\left(1-e^{-i\omega t}\right)\cdot G_{zz}(i\omega)\cdot|F_z(t)|\cdot e^{i\omega}\end{cases} \tag{5}$$

The relationship between Q-factor and damp ratio can be expressed as [48]

$$\xi=\frac{1}{2Q} \tag{6}$$

Then, the regenerative displacement in Eq. (5) can be expressed as

$$\begin{cases}\Delta x(i\omega t)=\dfrac{\left(1-e^{-i\omega t}\right)\cdot|F_x(t)|\cdot e^{i\omega}}{k_x\cdot\left[-\left(\frac{\omega}{\omega_x}\right)^2+\frac{i\omega}{Q_x\cdot\omega_x}+1\right]}\\ \Delta y(i\omega t)=\dfrac{\left(1-e^{-i\omega t}\right)\cdot|F_y(t)|\cdot e^{i\omega}}{k_y\cdot\left[-\left(\frac{\omega}{\omega_y}\right)^2+\frac{i\omega}{Q_y\cdot\omega_y}+1\right]}\\ \Delta z(i\omega t)=\dfrac{\left(1-e^{-i\omega t}\right)\cdot|F_z(t)|\cdot e^{i\omega}}{k_z\cdot\left[-\left(\frac{\omega}{\omega_z}\right)^2+\frac{i\omega}{Q_z\cdot\omega_z}+1\right]}\end{cases} \tag{7}$$

As expressed in Eq. (7), with the decrement of the Q-factor, the regenerative displacement becomes lower. The exchange of step response for the machine tool-workpiece system with respect to Q-factor in one direction is shown in Fig. 2. As is shown in Fig. 2, for the system with low Q-factors ($Q<1/2$), it is overdamped with no oscillation. On the contrary, the system with high Q-factor ($Q>1/2$) is underdamped and the system will oscillate with input of specified frequency. For the system with $Q=1/2$, it is a critical damped system. As the overdamped system, the critical system will not oscillate and it is not overshoot. Therefore, the change of modal parameters and the system response can be reflected with Q-factor.

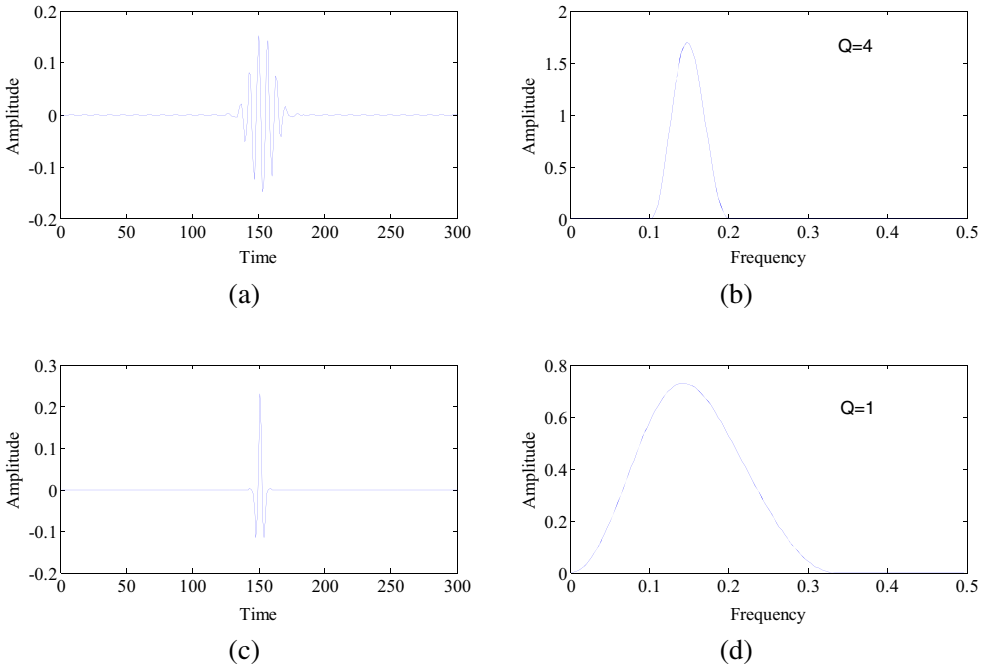

Fig. 1 Waveform and frequency response of signal with different oscillatory behavior. **a** Waveform of signal with $Q = 4$. **b** Frequency response of signal with $Q = 4$. **c** Waveform of signal with $Q = 1$. **d** Frequency response of signal with $Q = 1$

3 Linear predictive analysis for *Q*-factor precise calculation

Q-factor can be obtained with the principle of the linear predictive analysis. The main calculation procedure is expressed as follows [49]:

(1) Construct the auto-regressive model (AR model) with the measured signal as [50, 51]

$$x(n) = \sum_{k=1}^{p} a_k x(n-k) + Gu(n) \tag{8}$$

where p is the model order and $a_k$is the model coefficients. G is the gain coefficient. The transfer function of all-pole model can be formulated as

$$H(z) = \frac{G}{1 - \sum_{k=1}^{p} a_k z^{-k}} \tag{9}$$

(2) By substituting $z^{-1} = \exp(-j\omega T)$ or $z^{-1} = \exp(-j2\pi f/f_s)$ (f_s is the sampling frequency) into the transfer function and modulus operation and minimizing the prediction error in certain criterion, the model parameter of $\{a_k; k = 1, 2, \cdots p\}$ can be obtained through the Levinson-Durbin

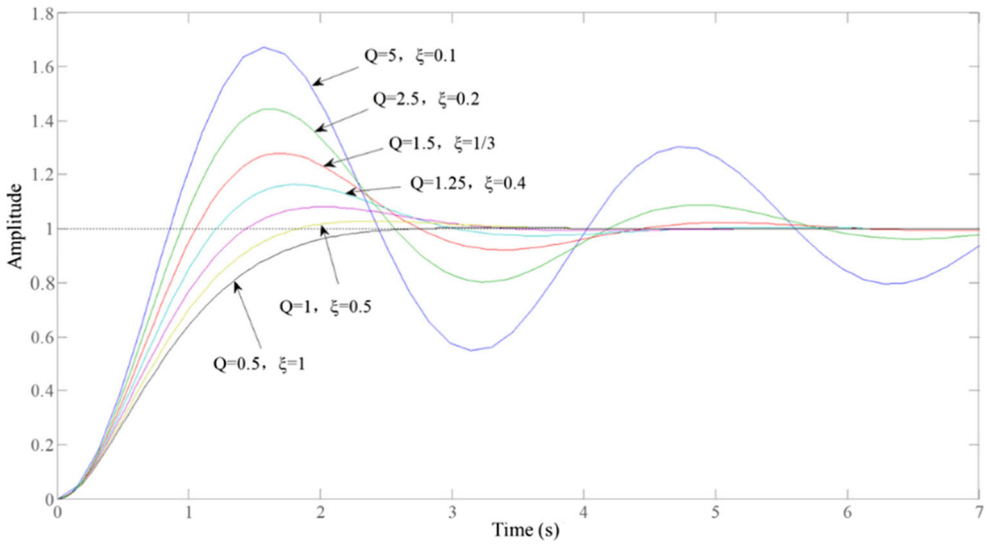

Fig. 2 Step response for the machine tool-workpiece system with variable Q-factor

algorithm [52]. Then, the power spectrum response can be obtained through the FFT of the prediction coefficients.

$$P(f) = |H(f)|^2 = \frac{G^2}{\left|1 - \sum_{k=1}^{p} a_k \exp(-j2\pi kf/fs)\right|^2} \tag{10}$$

(3) With the parabolic interpolation method, for every peak in the power spectrum response curve, the center frequency and corresponding bandwidth can be calculated. The parameters of the quadratic equations of $a_i\lambda^2 + b_i\lambda + c_i$ are obtained as

$$\begin{cases} a_i = (P_{m+1} + P_{m-1} - 2 \cdot P_m)/\Delta f^2 \\ b_i = (P_{m+1} + P_{m-1})/\Delta f^2 \\ c_i = P_m \end{cases} \tag{11}$$

where P_{m-1}, P_{m+1}, and P_m are the power spectrum values responding to point $m-1$, $m+1$, and local peak point m. Δf is the frequency space.

(4) Then the center frequency f_i and bandwidth Bw_i can be represented as

$$\begin{cases} f_i = (-b_i/2a_i + m)\Delta f \\ Bw_i = -\dfrac{\sqrt{b_i^2 - 4a_i(c_i - 0.5P_{si})}}{a_i} \times \Delta f \end{cases} \tag{12}$$

where $P_{si} = \frac{b_i^2}{4a_i} - \frac{b_i^2}{4a_i} + c_i = -\frac{b_i^2}{4a_i} + c_i$ is the parabolic interpolated power spectrum value through the derivation of quadratic equation, $d(a_i\lambda^2 + b_i\lambda + c_i)/d\lambda = 0$.

(5) With the calculating method, Q-factors of the jth frequency during cutting time of $\{i, i+n\}$ can be expressed as

$$Q_{i,j} = \frac{f_{i,j}}{Bw_{i,j}} \; i = 1, 2, \cdots N \;\; j = 1, 2, \cdots m \tag{13}$$

where m is the number of the spectral lines.

4 Experiment setup of thin-walled part milling

In order to illustrate the effectiveness of Q-factor, two typical thin-walled part machining processes, flank milling and mirror milling, were conducted.

4.1 Flank milling

The flank milling process was carried on a thin wall open geometry of a cantilever of 400 mm × 300 mm × 6 mm thick workpiece overhanging for a length of 41 mm, as is shown in Fig. 3, on a Mikron HSM 500 vertical machining center with a 4.2-kW, 42,000-rpm spindle. The material of the workpiece was aluminum alloy 7075. The parameters of the end mill are listed in Table. 1. The machining process maintained a constant cutting speed of 4000 rpm and feed rate of 400 mm/min with axial and radial depth of cut ($a_p = 0.5$ mm, $a_e = 5$ mm). In order to simulate the exchange of vibration modes, the bottom middle side of workpiece with length of 100 mm was fixed and flank milling proceeded along the long unfixed side. An eddy current displacement sensor (Keyence EX-V10) was mounted on the opposite of the cutting point to measure the vibration displacement signal with the sample frequency of 3000 Hz. The setup of thin-walled part machining and the measured vibration signal are shown in Fig. 3.

In order to describe the oscillatory characteristics in details, three signal segments and corresponding frequency spectrum with different machining states deriving from the measured vibration displacement signal are shown in Fig. 4. As is shown in Fig. 4a in the first 1 s of the machining time, the machining state was extremely unstable and the oscillatory characteristics of the signal were chaotic. The energy of the signal mainly distributed around the 257 Hz, and its corresponding bandwidth was wider. Besides, the cutting frequency of 267 Hz was shown in the frequency spectrum but it was not the dominant frequency. For the slight chatter state during machining time from 66.6 to 68.0 s, the vibration signal exhibited a certain degree of periodicity. In this case, the frequency of both 257 Hz and 267 Hz dominated the frequency spectrum. But the frequency bandwidth of 257 Hz became narrower obviously. For the machining time in the last 1 s of the machining time, the machining state was extremely unstable and the oscillatory characteristics of the signal was chaotic again. The energy of the signal mainly distributed around 257 Hz. And its corresponding bandwidth was wider again. Therefore, for the machining process from unstable to stable and then unstable, the energy and bandwidth of 257 Hz exhibited conspicuous exchange and can be regarded as the chatter-related signal component.

4.2 Mirror milling

Mirror milling has been an effective way for the stable manufacturing method of thin-walled parts [53]. In this paper, the mirror milling system (MMS), which is able to operate at a high speed (18,000 rpm), was developed for the mirror milling experiment. A thin-walled aluminum alloy 7075 plate with 1100 mm × 750 mm × 6 mm was vertically mounted on a fixture with only two sides fixed. Mirror milling was tested

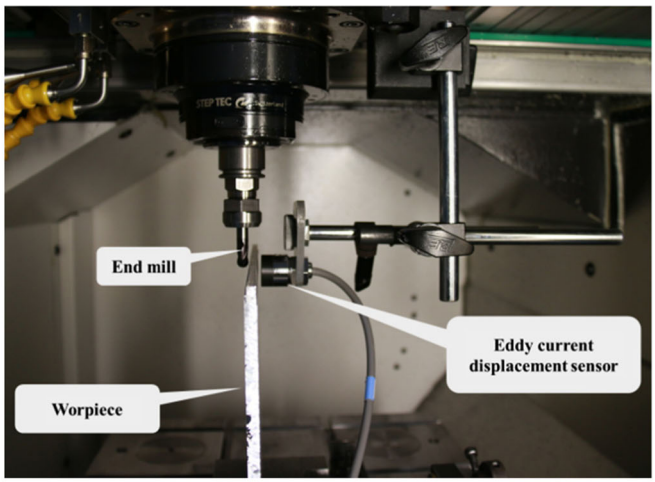

(a)

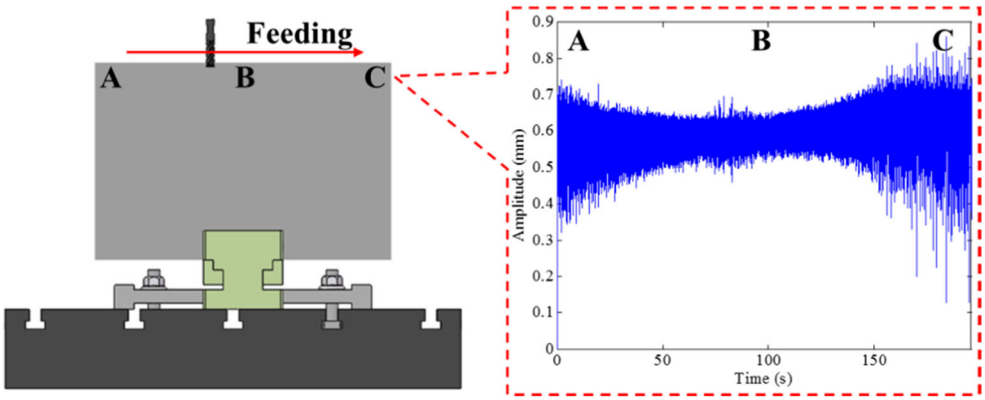

(b)

Fig. 3 Thin-walled part flank milling. **a** Setup. **b** Measured vibration signal

with the same end mill as was used in the flank milling, and the corresponding parameters are listed in Table. 1. A multi-component dynamometer (Kistler 9317C), coupled with charge amplifiers, was used to measure the supporting forces in three orthogonal directions (f_x, f_y, f_z). Three eddy current displacement sensors (Keyence EX-V10) were mounted around the dynamometer to measure the vibration displacement signal. The experimental setup is shown in Fig. 5.

Table 1 Parameters of the end mill

Symbols	Terminology	Values
γ	Helix angle (°)	30
γ_0	Rake angle (°)	13
r	Edge radius (mm)	0.4
A_p	Maximum cutting depth (mm)	15
D	Tool diameter (mm)	10
N	Number of flutes	4

As is shown in Fig. 5a, tests in slot milling were performed within a rectangular region of 80 mm × 80 mm on the thin-walled parts. The machining process maintained a constant cutting speed of 3000 rpm with axial and radial depth of cut ($a_p = 2$ mm, $a_e = 10$ mm). In the middle of the slot milling, the feed rate changed from 100 to 200 mm/min. The supporting force signal is shown in Fig. 5c. For the machining process with feed rate of 100 mm/min, the supporting force signal was relatively chaotic. At the boundary where the feed rate exchanged, the supporting force signal was obviously aperiodic. But then, the supporting signal became stable and periodic when the feed rate reached up to 200 mm/min. The reason for this can be explained that the cutting force in the axis direction increased with the increment of the feed rate and the restraint function between the cutter and workpiece was reinforced. Therefore, the vibration derived from the intermittent cutting of the cutter dropped off and the supporting force on the opposite side exhibited a certain degree of periodicity.

In order to describe the signal oscillatory characteristics in detail, three signal segments deriving from the measured

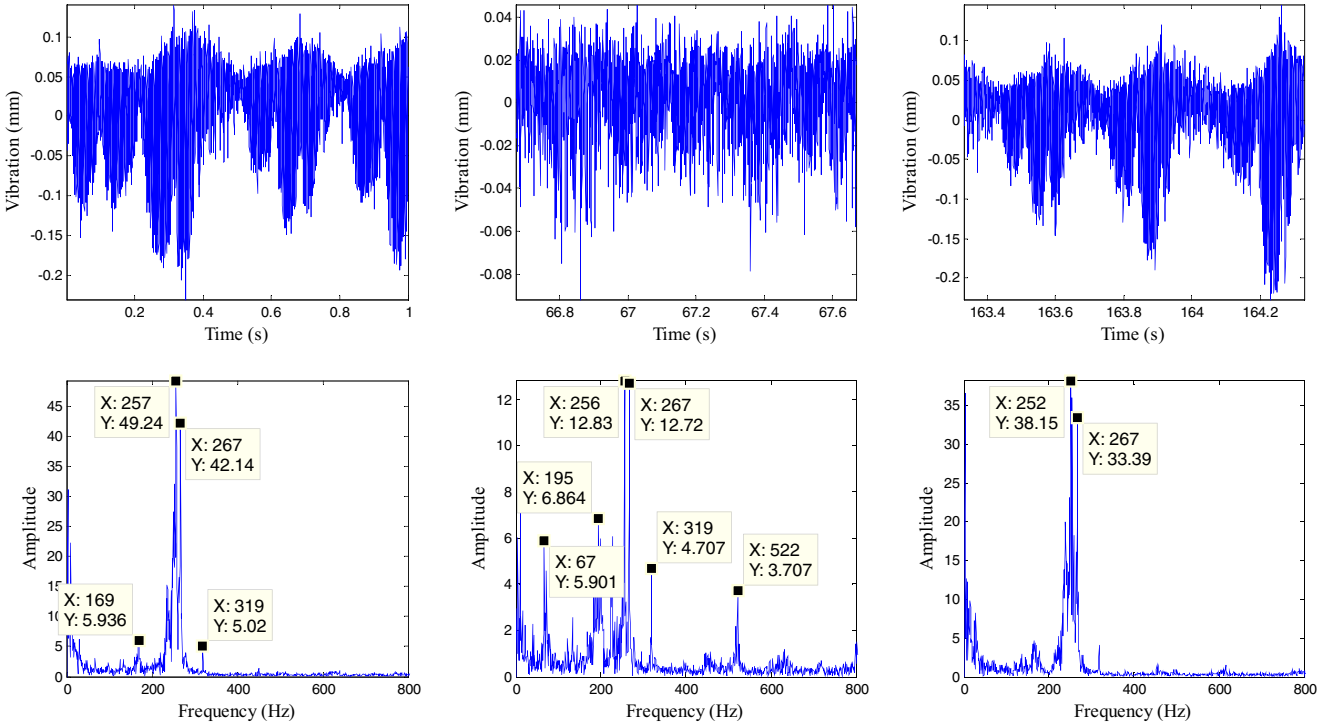

Fig. 4 Signal segments and corresponding main frequencies deriving from flank milling process

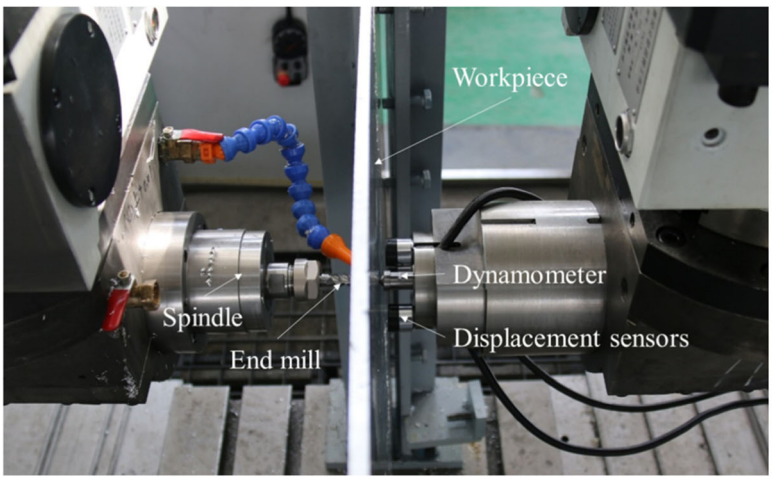

(a)

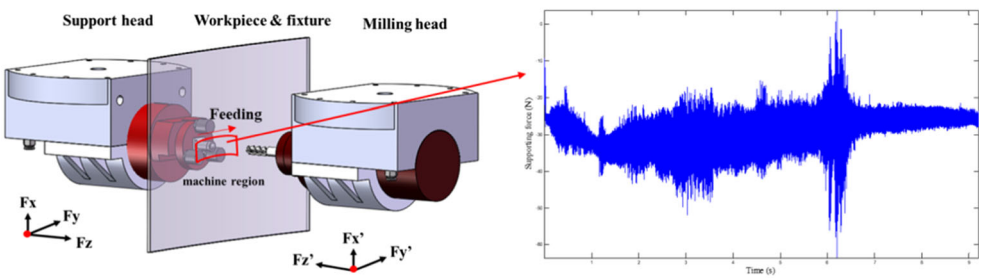

(b)

Fig. 5 Thin-walled parts mirror milling. **a** Setup. **b** Vibration signals by supporting force sensor

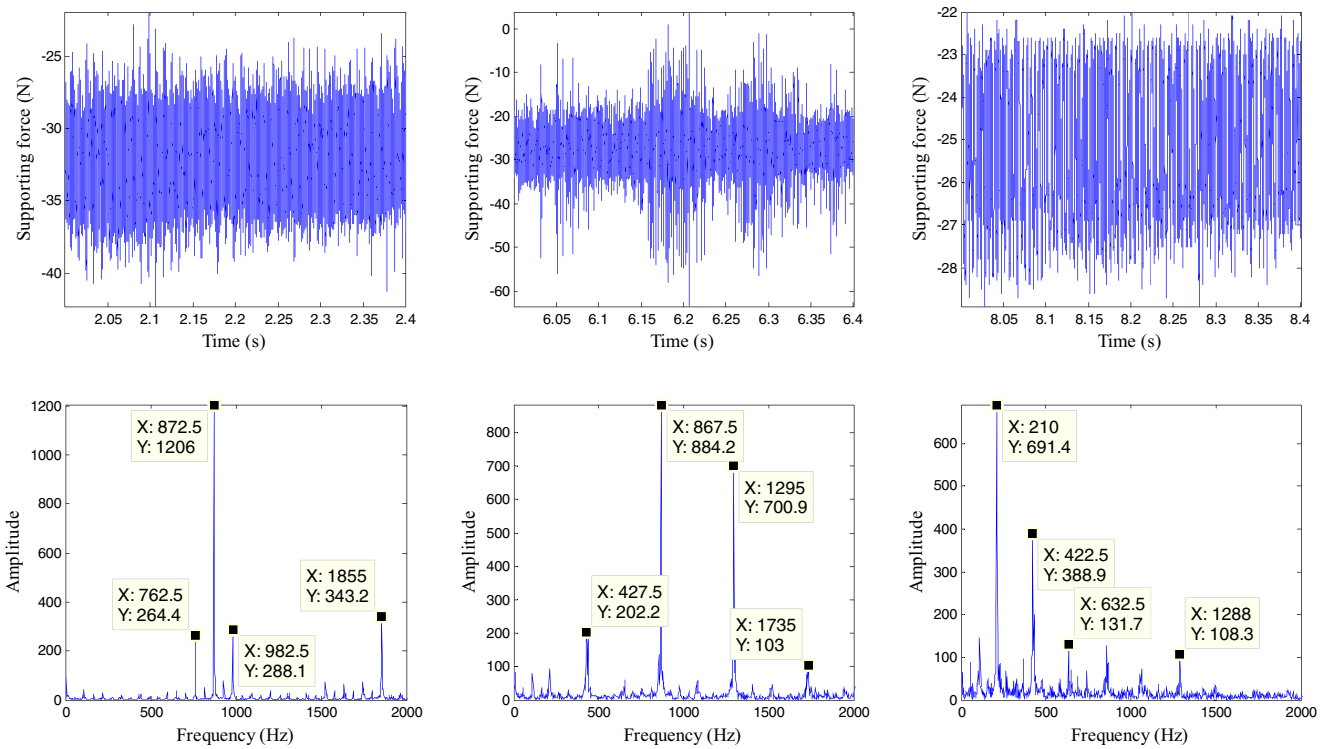

Fig. 6 Signal segments and corresponding main frequencies deriving from mirror milling process

supporting force and corresponding frequency spectrum are shown in Fig. 6. For the signal segments shown in Fig. 6a which derived from the machining time of the first 2.4 s, the signal was aperiodic and the signal energy mainly distributed around 872 Hz with a relative narrow bandwidth. For the signal segments shown in Fig. 6b which derived from the machining state exchange process, the signal was more aperiodic. For the signal segments in the last 2.4 s shown in Fig. 6c, the signal became periodic and the energy began to distribute around the spindle rotation frequency and its harmonics. Therefore, the frequency of 872 Hz was defined as the chatter-related signal component.

5 Chatter identification ability analysis using *Q*-factor

In this part, facing the two different thin-walled part machining processes, the common used time domain and time-frequency domain indicators were chosen to illustrate the chatter state of flank milling process and mirror milling process. The time domain indicators include standard deviation, root mean square, peak value, crest factor, coefficients of variation, kurtosis, energy of signal, impulse factor, skewness, clearance factor, and permutation entropy. The time-frequency domain indicators include power spectral entropy, complexity, spectral kurtosis, and *Q*-factors proposed in this paper. Their identification ability in terms of its ability to express characteristics of machining state, sensibility to the exchange of machining state, and chatter-related information inclusion was compared with the designed experiments.

The ability of indicators to express characteristics of machining state can be evaluated with the value of indicators. With the change of the machining state, the corresponding indictors should show relative variation with an obvious trend. And the variation should show a certain degree of correlation. The sensibility of the indicators to the change of machining state can be evaluated with value transform at the place where machining state exchanged. The chatter-related information inclusion refers to the physical meaning of the chosen indicator, i.e., it can not only reflect the change of modal parameters and locate the chatter-related signal component but also quantify the level of chatter.

5.1 Identification abilities in flank milling

For the flank milling process, the corresponding values of the time domain indicators and time-frequency domain indicators are shown in Fig. 7.

As is shown in Fig. 7, the time domain and time-frequency domain indicators showed relative variation with the flank milling process. The variation of these indicators can be roughly divided into four trends. For standard deviation, peak value, impulse factor, power spectral entropy, and complexity,

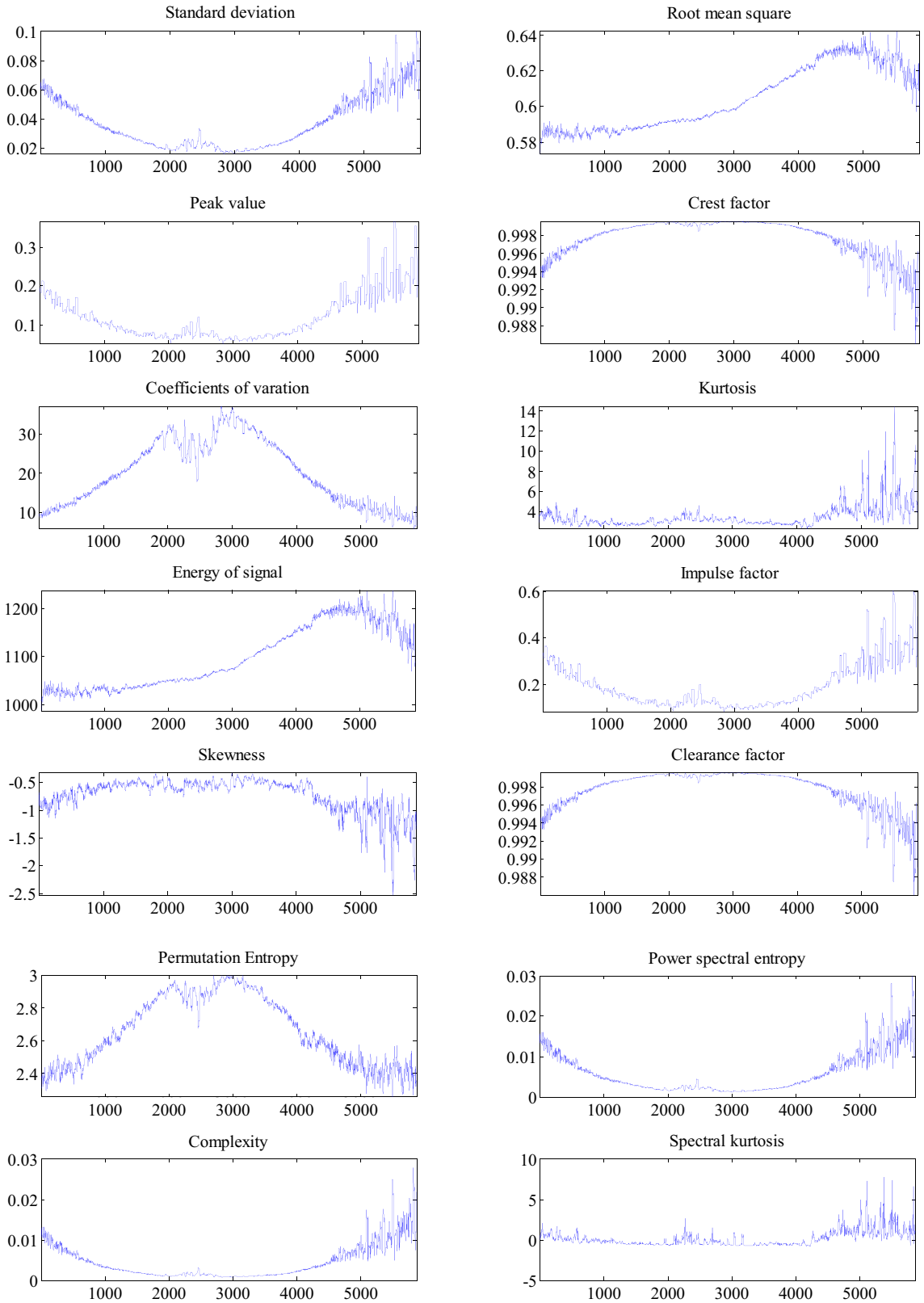

Fig. 7 The chatter indicators of vibration signal within flank milling process

the values were relatively higher in severe chatter state but lower in slight chatter state. But the variation of these indicators was in a slow trend. The variation in a slow trend will make the threshold setting difficult. Similarly, the crest

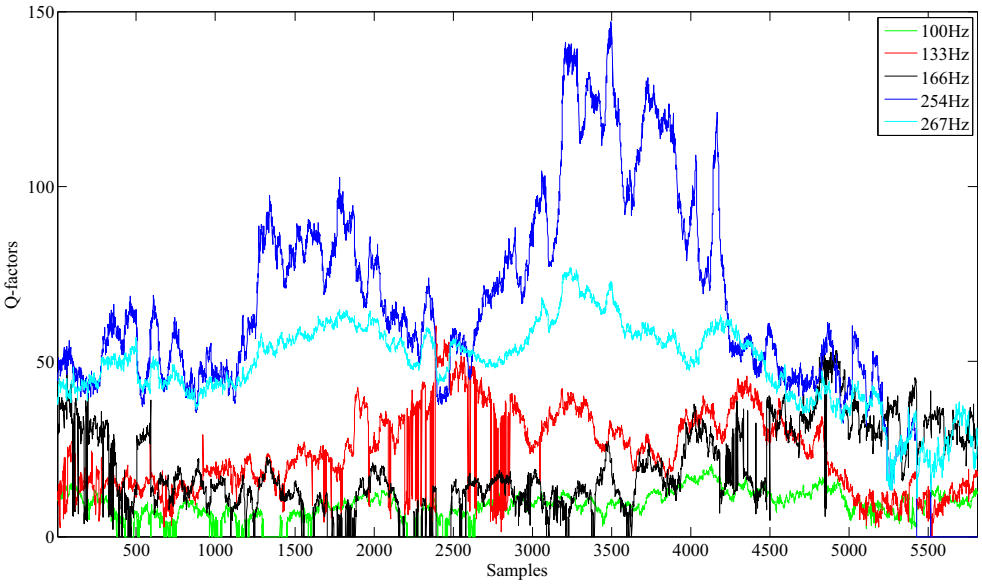

Fig. 8 *Q*-factors corresponding to different frequencies within flank milling process

factor, skewness, and clearance factor experienced a reverse exchange, i.e., lower in slight chatter state but higher in severe chatter state. The variation was also in a slow trend. For coefficients of variation and permutation entropy, the variation was in a fast trend, which would make the threshold setting easy. Another trend was exhibited by kurtosis and spectral kurtosis. They only showed a certain degree of increment at the end of the milling process but remained unchanged at the beginning and middle parts of the milling process. The similar trend was also exhibited by root mean square and energy of signal. Therefore, for the indicators mentioned above, they lacked the ability in expressing characteristics of machining state.

For the designed flank milling experiment, the place where machining state mutated was located at the critical point between the places where the parts were fixed and where they were unfixed. Therefore, an employable indicator should also have mutation near this place. As is shown in Fig. 7, although these indicators showed relative exchange within the machining process, there was no obvious mutation at the place where machining state exchanged. Based on the value of these indicators, it was difficult to locate the place where the chatter happened. Therefore, these indicators lacked the sensibility to the change of machining state.

As a multi-dimensional indicator, *Q*-factors corresponding to the dominant frequencies (the chatter-related frequency 254 Hz and the harmonics of spindle rotation frequency 100 Hz, 133 Hz, 166 Hz, 266 Hz) are shown in Fig. 8. As is shown in Fig. 8, the *Q*-factors of 100 Hz, 133 Hz, 166 Hz, and 266 Hz experienced a relative gentle variation process. Compared with the *Q*-factors of these frequencies, the *Q*-factors of 254 Hz exhibited more violent variation process. At the beginning and end of the machining process where the machining state was unstable, *Q*-factors were relatively low. But at the middle of the machining process where the machining state was stable, the *Q*-factor was relatively high. Besides, *Q*-factors corresponding to frequency of 254 Hz climbed steeply at the place where machining state changed from unstable to stable and declined steeply at the place where machining state changed from stable to unstable.

Therefore, for thin-walled parts flank milling process, *Q*-factor of the chatter-related signal component showed perfect ability to express characteristics of machining state and more sensitivity to the change of machine state. Besides, it included the information about center frequency and oscillatory characteristics of multiple dominant frequencies. The center frequency 254 Hz could be used for chatter-related signal component identification, and the value of 254 Hz could be used to quantify the level of chatter.

5.2 Identification abilities in mirror milling

For the mirror milling process, the corresponding values of the time domain indicators and time-frequency domain indicators are shown in Fig. 9. It was clearly shown that there was obvious enlargement at the place where feed rate changed from 100 to 200 mm/min for standard deviation, peak value, impulse factor, power spectral entropy, and complexity. For crest factor and clearance factor, they experienced a reverse exchange. For coefficients of variation, kurtosis, and spectral kurtosis, the enlargement at the place where machining state changed was not as significant as the indicators mentioned above. But the corresponding values of these indicators in stable state and unstable state were at the same level. It was difficult to identify if there was chatter or not with these indicators. Therefore, these indicators showed a certain degree of sensibility to the change of machining state but limited ability to express the exchange of machining state.

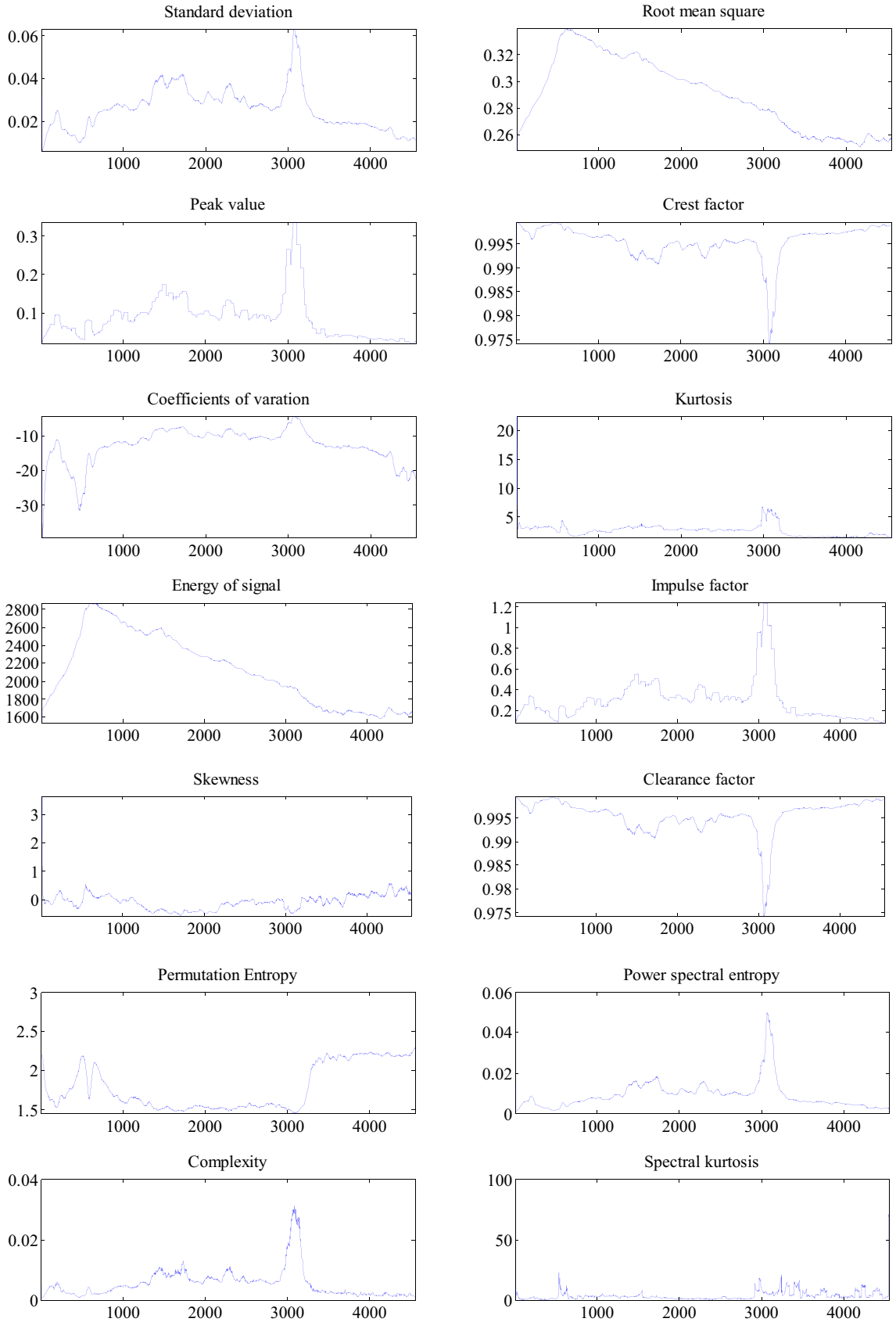

Fig. 9 The chatter indicators of vibration signal within mirror milling process

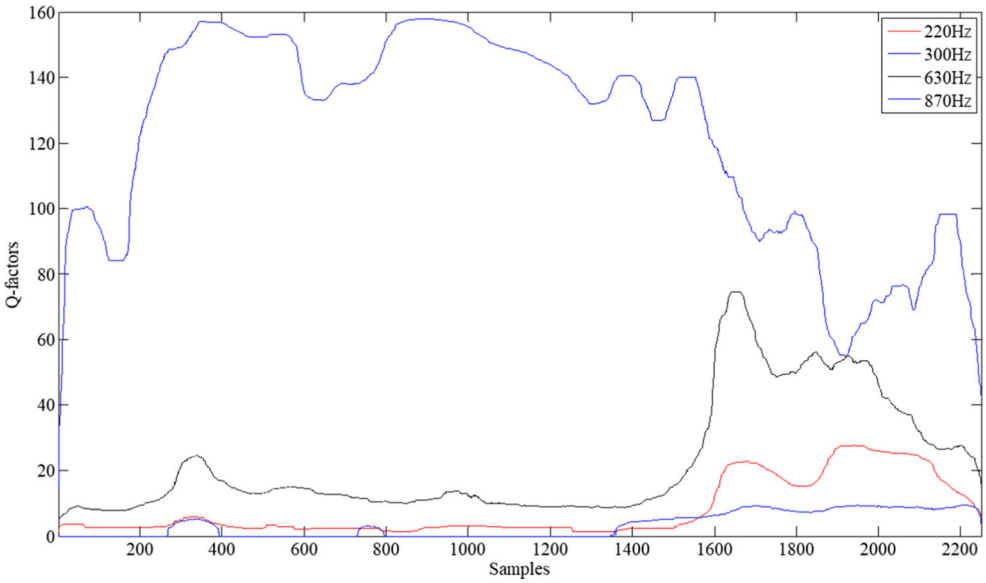

Fig. 10 *Q*-factors corresponding to different frequencies within mirror milling process

Besides, it should be noted that for the mirror milling process, permutation entropy showed excellent performance in machining state identification. The value of permutation entropy remained at a low level for the unstable state but spurted when the feed rate changed from 100 to 200 mm/min. But compared with the flank milling process shown in Fig. 7, the indicative function of permutation entropy was limited.

Q-factors corresponding to different frequencies are shown in Fig. 10. As is shown in Fig. 10, the *Q*-factors corresponding to frequency of 872 Hz reduced dramatically at the place where machining state changed. But for *Q*-factors corresponding to frequency of 220 Hz, 300 Hz, and 630 Hz, their values increased slightly at the place where machining state changed. This phenomenon indicated that with the increment of the feed rate, the energy of the measured signal began to distribute around the spindle rotation frequency and its couplings. With the change of the *Q*-factors, the frequency of 872 Hz can be identified as the chatter-related signal component and the corresponding value of *Q*-factors can be used for quantifying the level of chatter. Therefore, for mirror milling process, *Q*-factors showed excellent ability to express the exchange of machining state and made great contribution to the threshold setting for machining state identification. The obvious mutation at the place where machining state changed showed sensibility of *Q*-factors to the exchange of machining state, which will be extremely useful in the machining state identification.

6 Conclusions

In this paper, a novel chatter indicator, *Q*-factor, was proposed to identify the machining state and its identification ability was analyzed. In order to illustrate the effectiveness of the proposed indicator, the relationship between *Q*-factor and the signal oscillatory behavior was elaborated from the perspective of signal's time-frequency characteristic and tool-workpiece system's response. The comparison between two different thin-walled part machining processes, i.e., flank milling and mirror milling, in the aspects of ability to express characteristics of machining state, sensibility to the change of machining state, and chatter-related information inclusion between time domain indicators, time-frequency domain indicators, and *Q*-factors was conducted. The comparison between the two different machining methods shows that:

(1) The value of *Q*-factor exhibits obvious difference between stable state and chatter state and shows excellent ability to express the exchange of machining state. The obvious difference makes great contribution to the threshold setting for machining state identification.
(2) There was obvious mutation at the place where the machining state changed. The obvious increment or reduction of *Q*-factor can be a useful indicator which will supply more useful and effective information for the following chatter prediction and suppression before the chatter is completely developed.
(3) *Q*-factor is a multi-dimensional indicator, including the information about center frequency and oscillatory characteristics of multiple dominant frequencies. The center frequency can be used for chatter-related signal component identification, and the value can be used to quantify the level of chatter. The chatter information inclusion can be helpful in chatter-related signal identification based on the *Q*-factor variation.

The potential application of the Q-factor can be extended to fault diagnosis of rotary machineries, like bearings, gears, and so on.

Funding information This work is supported by National Basic Research Program Funding Agency of China (Grant No. 2014CB046604), by the Fundamental Research Funds for the Central Universities (Grant No. DUT17JC16), and by Open Research Fund of Key Laboratory of High Performance Complex Manufacturing, Central South University (Grant No. Kfkt2016-05).

References

1. Quintana G, Ciurana J (2011) Chatter in machining processes: a review. Int J Mach Tools Manuf 51:363–376
2. Lamraoui M, Thomas M, Badaoui ME, Girardin F (2014) Indicators for monitoring chatter in milling based on instantaneous angular speeds. Mech Syst Signal Process 44:72–85
3. Hu CQ, Smith WA, Randall RB, Peng ZX (2016) Development of a gear vibration indicator and its application in gear wear monitoring. Mech Syst Signal Process 76-77:319–336
4. Davies MA, Balachandran B (2000) Impact dynamics in milling of thin wall structures. Nonlinear Dyn 22:375–392
5. Lai GJ, Chang JY (1995) Stability analysis of chatter vibration for a thin-wall cylindrical workpiece. Int J Mach Tools Manuf 35:431–444
6. Yan ZH, Liu ZB, Wang XB, Liu B, Luo ZW, Wang DQ (2016) Stability prediction of thin-walled workpiece made of Al7075 in milling based on shifted Chebyshev polynomials. Int J Adv Manuf Technol 87:1–10
7. Campa FJ, Lacalle LNLD, Celaya A (2011) Chatter avoidance in the milling of thin floors with bull-nose end mills: model and stability diagrams. Int J Mach Tools Manuf 51:43–53
8. Atlar S, Budak E, Özgüven HN (2008) Modeling part dynamics and chatter stability in machining considering material removal
9. Luo M, Zhang DH, Wu BH, Tang M (2011) Modeling and analysis effects of material removal on machining dynamics in milling of thin-walled workpiece. Adv Mater 223:671–678
10. Alan S, Budak E, Özgüven HN (2010) Analytical prediction of part dynamics for machining stability analysis. Int J Automat Technol 4
11. Song QH, Liu ZQ, Wan Y, Ju GG, Shi JH (2015) Application of Sherman–Morrison–Woodbury formulas in instantaneous dynamic of peripheral milling for thin-walled component. Int J Mech Sci 96–97:79–90
12. Wang L, Liang M (2009) Chatter detection based on probability distribution of wavelet modulus maxima. Robot Comput Integr Manuf 25:989–998
13. Sick B (2002) On-line and indirect tool wear monitoring in turning with artificial neural networks: a review of more than a decade of research. Mech Syst Signal Process 16:487–546
14. Dong J, Subrahmanyam KVR, Wong YS, Hong GS, Mohanty AR (2006) Bayesian-inference-based neural networks for tool wear estimation. Int J Adv Manuf Technol 30:797–807
15. Salgado DR, Alonso FJ (2006) Tool wear detection in turning operations using singular spectrum analysis. J Mater Process Technol 171:451–458
16. Kim HY, Ahn JH (2002) Chip disposal state monitoring in drilling using neural network based spindle motor power sensing. Int J Mach Tools Manuf 42:1113–1119
17. Zhu K, Wong YS, Hong GS (2009) Multi-category micro-milling tool wear monitoring with continuous hidden Markov models. Mech Syst Signal Process 23:547–560
18. Binsaeid S, Asfour S, Cho S, Onar A (2009) Machine ensemble approach for simultaneous detection of transient and gradual abnormalities in end milling using multisensor fusion. J Mater Process Technol 209:4728–4738
19. Dron JP, Bolaers F, Rasolofondraibe L (2004) Improvement of the sensitivity of the scalar indicators (crest factor, kurtosis) using a de-noising method by spectral subtraction: application to the detection of defects in ball bearings. J Sound Vib 270:61–73
20. Fu Y, Zhang Y, Zhou HM, Li DQ, Liu HQ, Qiao HY, Wang XQ (2016) Timely online chatter detection in end milling process. Mech Syst Signal Process 75:668–688
21. Al-Ghamd AM, Mba DA (2006) Comparative experimental study on the use of acoustic emission and vibration analysis for bearing defect identification and estimation of defect size. Mech Syst Signal Process 20:1537–1571
22. Zhang H, Chen XF, Du ZH, Yan RQ (2016) Kurtosis based weighted sparse model with convex optimization technique for bearing fault diagnosis. Mech Syst Signal Process 80:349–376
23. Al-Habaibeh A, Gindy N (2000) A new approach for systematic design of condition monitoring systems for milling processes. J Mater Process Technol 107:243–251
24. Choi T, Shin YC (2003) On-line chatter detection using wavelet-based parameter estimation. J Manuf Sci Eng 125:21–28
25. Bhattacharyya P, Sengupta D, Mukhopadhyay S (2007) Cutting force-based real-time estimation of tool wear in face milling using a combination of signal processing techniques. Mech Syst Signal Process 21:2665–2683
26. Teti R, Jemielniak K, O'Donnell G, Dornfeld D (2010) Advanced monitoring of machining operations. CIRP Ann Manuf Technol 59:717–739
27. Lamraoui M, Barakat M, Thomas M, Badaoui ME (2015) Chatter detection in milling machines by neural network classification and feature selection. J Vib Control 21:1251–1266
28. Ren JB, Sun GZ, Chen B, Luo M (2015) Multi-scale permutation entropy based on-line milling chatter detection method. J Mech Eng 51:206
29. Nair U, Krishna BM, Namboothiri VNN, Nampoori VPN (2010) Permutation entropy based real-time chatter detection using audio signal in turning process. Int J Adv Manuf Technol 46:61–68
30. Marinescu I, Axinte DA (2008) A critical analysis of effectiveness of acoustic emission signals to detect tool and workpiece malfunctions in milling operations. Int J Mach Tools Manuf 48:1148–1160
31. Jemielniak K (2000) Some aspects of AE application in tool condition monitoring. Ultrasonics 38:604–608
32. Maggioni M, Marzorati E, Grasso M, Colosimo BM (2014) In-process quality characterization of grinding processes: a sensor-fusion based approach. ASME Biennial Conference on Engineering Systems Design, Esda, pp 1–2
33. Cao H, Zhou K, Chen X (2015) Chatter identification in end milling process based on EEMD and nonlinear dimensionless indicators. Int J Mach Tools Manuf 92:52–59
34. Antoni J (2006) The spectral kurtosis: a useful tool for characterising non-stationary signals. Mech Syst Signal Process 20:282–307
35. Chen BQ, Zhang ZS, Zi YY, He ZJ, Sun C (2013) Detecting of transient vibration signatures using an improved fast spatial–spectral ensemble kurtosis kurtogram and its applications to mechanical signature analysis of short duration data from rotating machinery. Mech Syst Signal Process 40:1–37
36. Wang YX, Liang M (2011) An adaptive SK technique and its application for fault detection of rolling element bearings. Mech Syst Signal Process 25:1750–1764

37. Yang Y, YuDejie CJS (2006) A roller bearing fault diagnosis method based on EMD energy entropy and ANN. J Sound Vib 294:269–277
38. Liu C, Zhu L, Ni C (2017) The chatter identification in end milling based on combining EMD and WPD. Int J Adv Manuf Technol 91: 3339–3348
39. Shao H, Shi X, Li L (2011) Power signal separation in milling process based on wavelet transform and independent component analysis. Int J Mach Tools Manuf 51:701–710
40. Plaza EG, López PJN (2017) Surface roughness monitoring by singular spectrum analysis of vibration signals. Mech Syst Signal Process 84:516–530
41. Hu CZ, Yang Q, Huang MY, Yan WJ (2017) Sparse component analysis-based under-determined blind source separation for bearing fault feature extraction in wind turbine gearbox. IET Renew Power Gener 11:330–337
42. Zhong ZM, Chen J, Zhong P, Wu JB (2006) Application of the blind source separation method to feature extraction of machine sound signals. Int J Mach Tools Manuf 28:855–862
43. Cai GG, Chen XF, He ZJ (2013) Sparsity-enabled signal decomposition using tunable Q-factor wavelet transform for fault feature extraction of gearbox. Mech Syst Signal Process 41:34–53
44. Selesnick IW (2011) Resonance-based signal decomposition: a new sparsity-enabled signal analysis method. Signal Process 91:2793–2809
45. Shi JJ, Liang M (2016) Intelligent bearing fault signature extraction via iterative oscillatory behavior based signal decomposition (IOBSD). Expert Syst Appl 45:40–55
46. Wang HC, Chen J, Dong GM (2014) Feature extraction of rolling bearing's early weak fault based on EEMD and tunable Q-factor wavelet transform. Mech Syst Signal Process 48:103–119
47. Wang M, Gao L, Zheng Y (2014) Prediction of regenerative chatter in the high-speed vertical milling of thin-walled workpiece made of titanium alloy. Int J Adv Manuf Technol 72:707–716
48. Siebert WM (1986) Circuits, signals, and systems. MIT Press 86: 21–134
49. Wang YQ, Bo QL, Liu HB, Lian M, Wang F, Zhang J (2017) Full-oscillatory components decomposition from noisy machining vibration signals by minimizing the Q-factor variation. Trans Inst Meas Control 39(9):1313–1328
50. Polito F, Petri A, Pontuale G, Dalton F (2010) Analysis of metal cutting acoustic emissions by time series models. Int J Adv Manuf Technol 48:897–903
51. Aghdam BH, Vahdati M, Sadeghi MH (2015) Vibration-based estimation of tool major flank wear in a turning process using ARMA models. Int J Adv Manuf Technol 76:1631–1642
52. Levinson N (1946) The Wiener (root mean square) error criterion in filter design and prediction. J Math Phys 25:261–278
53. Lan J, Lin B, Huang T, Xiao JL, Zhang XF, Fei JX (2017) Path planning for support heads in mirror-milling machining system. Int J Adv Manuf Technol 91:617–628